

Orbital Mechanics
Dipartimento di Scienze e Tecnologie Aeroespaziali
Politecnico di Milano

ORBITAL MECHANICS PROJECT

Group 37
SINA ES HAGHI 952194 10693213
GIULIA SALA 968416 10582449
VALERIO SANTOLINI 968412 10568153
PIETRO ZORZI 969225 10607053



A.Y. 2020/21

Contents

1	Interplanetary explorer mission	1
1.1	Preliminary analysis	1
1.2	Synodic period	2
1.3	Algorithm	3
1.4	Find the optimum trajectory	5
1.4.1	The main program script	5
1.4.2	The optimization script	6
1.5	Results analysis	7
1.5.1	Departure from planet Earth	8
1.5.2	Arrival at planet Mercury	8
1.5.3	Flyby and Gravity Assist at planet Venus	9
2	Planetary Mission Design	10
2.1	Groundtracks analysis	10
2.1.1	Groundtrack and Earth's oblateness effects	10
2.1.2	The Repeating Groundtrack	11
2.2	Perturbed Orbit Propagation	12
2.2.1	Perturbed Problem	13
2.2.1.1	Oblateness Effects	13
2.2.1.2	Solar Radiation Pressure Effects	14
2.2.2	Combined effects	15
2.3	Comparison with Real Data	16
3	Conclusions	19
4	References	20

1. Interplanetary explorer mission

The objective of this section is to minimize the ΔV required by a spacecraft to perform its mission in a given time window. The transfer consists of an interplanetary travel from Earth to Mercury, performing a flyby at Venus to reduce costs. This chapter outlines the procedure used to obtain the preliminary feasibility analysis for the mission, beginning from the first estimates using approximated models and concluding with the results obtained with a Lambert problem solver and data from the ephemerides. Additionally, the procedure followed uses the patched conics method, considering three different restricted two-body problems for the different phases of the mission:

- interplanetary leg in heliocentric orbit from Earth to Venus;
- Flyby around Venus inside the planet's Sphere of influence;
- interplanetary leg in heliocentric orbit from Venus to Mercury.

1.1 Preliminary analysis

Considering the three planets of interest the spacecraft will need to reduce its velocity to lower the perihelion such that its trajectory can intersect Venus's orbital path, from where, slowing down further, it can proceed on towards Mercury. The following table presents the orbital elements of interest [1]:

Table 1.1: Planetary data.

Planet	Earth	Venus	Mercury
Inclination [deg]	0°	3.395°	7.005°
Eccentricity	0.0167	0.0067	0.205
Orbit period [days]	365.242	224.695	87.968
Semi-major axis [10^6 km]	149.596	108.209	57.909

To obtain a first esteem of the requirements in terms of ΔV it is possible to consider a Hohmann transfer, directly from Earth to Mercury, which can be considered on coplanar, coaxial and circular orbits. These hypotheses are justified as they are being used just to find a reference value and to better understand the procedure which will be refined later. Furthermore, the Earth belongs to the ecliptic plane and has a low value of eccentricity, so only Mercury's values are consistently different from the real ones.

By comparing the orbit semi-major axes of the three planets, it is easily acknowledged that Bi-elliptic transfer would not be more efficient than Hohmann.

To evaluate the ΔV required for the Hohmann transfer it is necessary to characterize the elliptical transfer orbit, in terms of specific angular momentum, h , which can be found from the semi-major axis of the two orbits. The velocity at apohelion and perihelion can be evaluated from h and by taking the difference with Earth's and Mercury's velocity respectively, the required ΔV for Hohmann transfer with the presented hypotheses is then:

$$\Delta V = \Delta V_{\text{Earth}} + \Delta V_{\text{Mercury}} = 17.144 \text{ km/s} \quad (1.1)$$

1.2 Synodic period

To better understand the possible optimal departure and arrival times it is useful to build two contour plots, also known as porkchop plots, which use real data from the ephemerides¹ and the Lambert solver to find the ΔV requirements for the transfers.

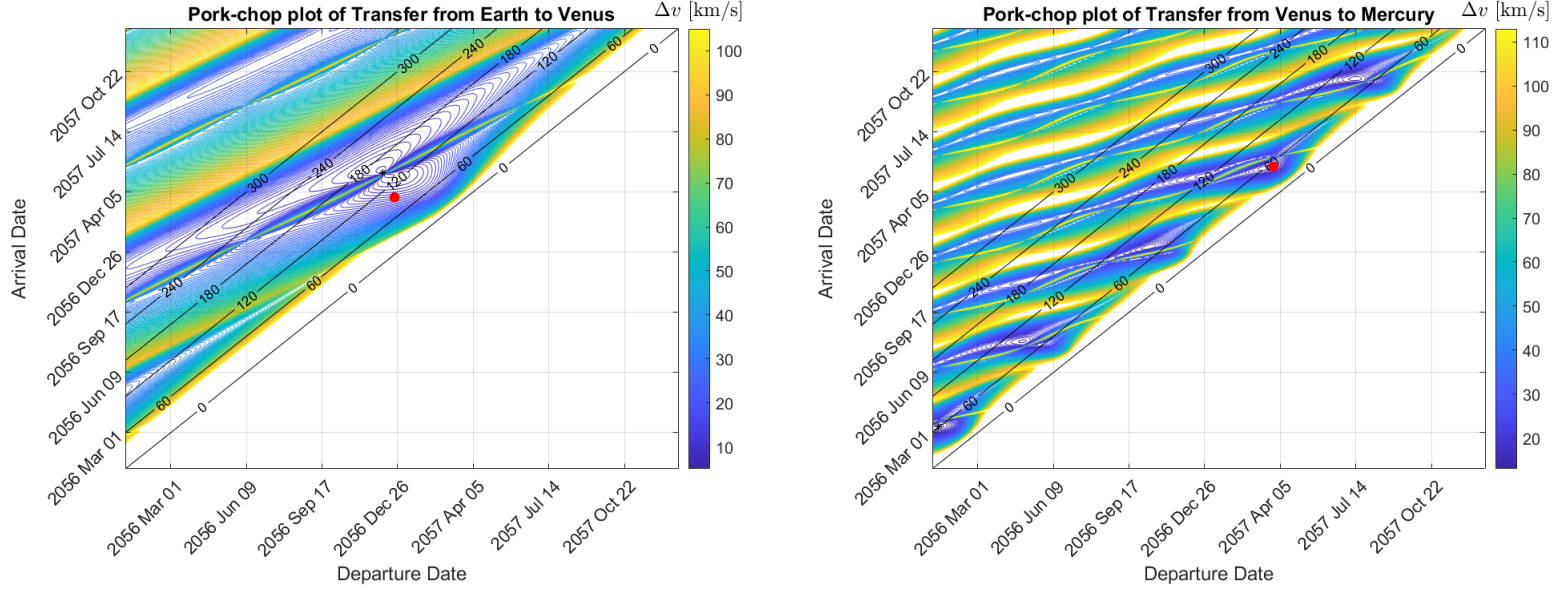


Figure 1.1: On the left, contour plot of transfer from Earth to Venus. On the right, contour plot of transfer from Venus to Mercury.

The red dots in the figures above represent the time configuration for the designed optimum trajectory, as explained later. The porckchop plots clearly show that the minimum cost for the transfers repeats at finite intervals of time which are nothing else than the synodic period between the considered celestial bodies. The graphs represent a limited time span of the entire window, since they repeat over time with minor differences. The synodic periods can be found analytically using the following formula:

$$T_{syn} = \frac{T_1 \times T_2}{|T_1 - T_2|} \quad (1.2)$$

$$T_{syn1} = 583.919 \text{ days} \quad (1.3)$$

$$T_{syn2} = 144.565 \text{ days} \quad (1.4)$$

Where T_{syn1} is refers to Earth-Venus and T_{syn2} refers to Venus-Mercury.

By taking the ratio between the two periods it can be shown that for every optimal transfer from Earth to Venus there are four optimal transfers from Venus to Mercury. Though, it is important to notice that the presented plots consider both the required variations of velocity at departure and arrival, the mission instead does not require manoeuvres to reach the orbit of the second planet. Furthermore the spacecraft performs a flyby that further reduces the necessary ΔV .

¹taken from uplanet.m

Moreover, as one can see in the plots, the optimal transfers are not perfectly matched, meaning that the arrival date at Venus requiring the least amount of ΔV is not the same of an optimal departure for Mercury, it is reasonable to assume that the final result will have the departure times near the minima of the two porkchop plots.

1.3 Algorithm

The main algorithm is an iterative process that is used to find the best solution using nested cycles, a powered gravity assist solver and the Lambert solver together to obtain the results. This process includes three loop-in-loops that in each loop, one of the time characteristics (departure, flyby, or arrival time) is changed within the given time interval using specified time steps.

To calculate the required velocity change in the first heliocentric leg, the position and velocity of planet Earth at the departure time is calculated. Then the position and the velocity of Venus at the time of flyby is calculated. For the Lambert solver, the position of planet Earth at departure time and the position of Venus at flyby time are given as initial and final arc point inputs, and the time difference between the flyby and departure is given as the time-of-flight input. The Lambert solver is set to provide the transfer arc and initial and final velocity for zero orbit revolution. From the difference between the initial velocity of the Lambert solver and the velocity of planet Earth, the required velocity change to get on the first heliocentric leg is computed. The difference between the final velocity of the Lambert arc and the velocity of Venus will be used later as entry velocity to calculate the powered gravity assist.

A similar method is used for the second heliocentric leg of the spacecraft's trajectory. Position and velocity of Mercury are calculated at arrival time. Then, the Lambert solver is used to find a transfer arc between Venus and Mercury and between the flyby and arrival time. The difference between the final velocity found by the Lambert solver and the velocity of Mercury will be the required velocity change of the second leg. The difference between the initial velocity in the Lambert arc and the velocity of Venus at the time of flyby will be used as the exit velocity in the powered gravity assist function.

For the powered gravity assist function, the entry and exit velocities are taken as the main inputs. Then the turn angle of the flyby hyperbola is calculated, and the periapsis radius of the hyperbola is computed through the “*Fsolve*” function. By having the hyperbola periapsis, the required velocity change at the periapsis for the powered gravity assist is found. Furthermore, the possibility of the spacecraft entering the atmosphere of Venus or impacting Venus itself is checked for every hyperbola to prove the feasibility of the flyby trajectory. The iterative algorithm process is explained in the flowchart of Figure (1.2).

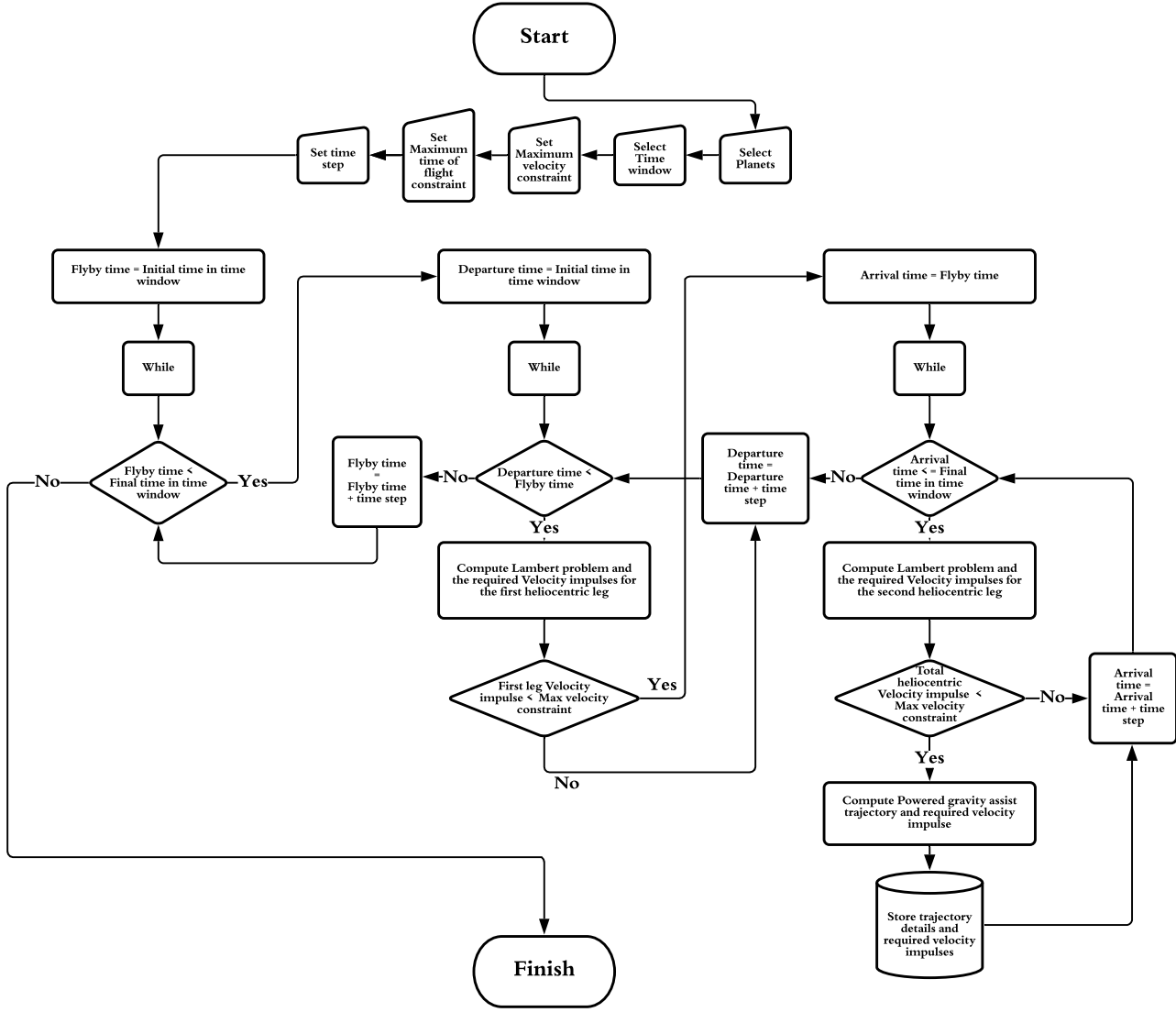


Figure 1.2: The script algorithm of the iterative process, consisting of three loops (while function).

Adopting this iteration algorithm for the whole duration of the time window is very time consuming (especially the “*Fsolve*” function in the powered gravity assist script). Logically, to increase the computation speed, higher time steps can be considered. However, since the orbital period of Mercury is around 88 days, even time steps as low as 10 days may skip good results. Therefore, the time step of five days was chosen for the iteration runs. To make the computations faster, three additional constraints are used:

- *Constraining the sum of heliocentric velocity changes ($\Delta V_{\text{Heliocentric-legs}}$):* In each full iteration, before solving the powered gravity assist, the required velocity changes for heliocentric legs are calculated and compared with a known minimum total velocity change ($\Delta V_{\text{tot,min}}$). The known minimum total velocity change can be considered as a constraint of the maximum allowed velocity in the program (ΔV_{max}). Iterations that have higher velocity change than the ΔV_{max} are discarded, and a new

iteration of the loop will be processed. The value of ΔV_{max} can be changed in the program based on decision and the better results that have been found.

- Using small time window: Instead of implementing the iteration process throughout the 40-year time interval, a smaller time window can be chosen.
- Constraining the maximum time of flight (ToF_{max}): Through constraining the maximum time difference between the time of departure and time of arrival, we can increase the speed of the computations.

1.4 Find the optimum trajectory

By employing the data provided from the preliminary analysis, a good estimation for the synodic period of Earth-Venus-Mercury system, and the known minimum heliocentric velocity change is found and used as the constraints for the initial program run.

- The initial $\Delta V_{max} = 17.2 \text{ km/s}$
- Time window = 2 years (more than the approximate synodic period)
- $ToF_{max} = 2 \text{ years}$ (since we are considering not to have any complete revolutions in our trajectory)

1.4.1 The main program script

For the initial program run, any 2-year time window in between the objective time interval can be chosen and the minimum approximate ΔV_{tot} can be computed for that time window (which will be the minimum ΔV_{tot} in the considered synodic period). Since in the real case, the planets are not on circular and coplanar orbits, the minimum ΔV_{tot} between different 2-year time windows may not be the same. Thus, with the new minimum ΔV_{tot} calculated in the previous step introduced as the new constraint on ΔV_{max} , and the defined ToF_{max} , the iterations can run for the complete duration of the given time window with pace and result in a new minimum ΔV_{tot} and the corresponding dates with respect to the designated time step of five days.

The initial run was carried out for the time window of December 1st, 2036 to December 1st, 2038 with the ΔV_{max} constraint of 17.2 km/s. The best result was of a trajectory with a ΔV_{tot} of 14.3 km/s. Afterwards, the program ran for the time window of December 1st, 2028 to December 1st, 2068 with the ΔV_{max} constraint of 14.3 km/s and the ToF_{max} of 2 years. All the data regarding the trajectories with ΔV_{tot} less than the ΔV_{max} constraint, were stored in several matrices.

The rows of the matrices contain the data of the trajectory in that iteration and each column index (or also called iteration index) of these matrices corresponds to a specific iteration configuration. Meaning that each column index represents a unique combination of a departure, flyby, and arrival times.

In Figure (1.3) the ΔV_{tot} of the trajectories in the second run of the program are plotted with respect to the designated column index.

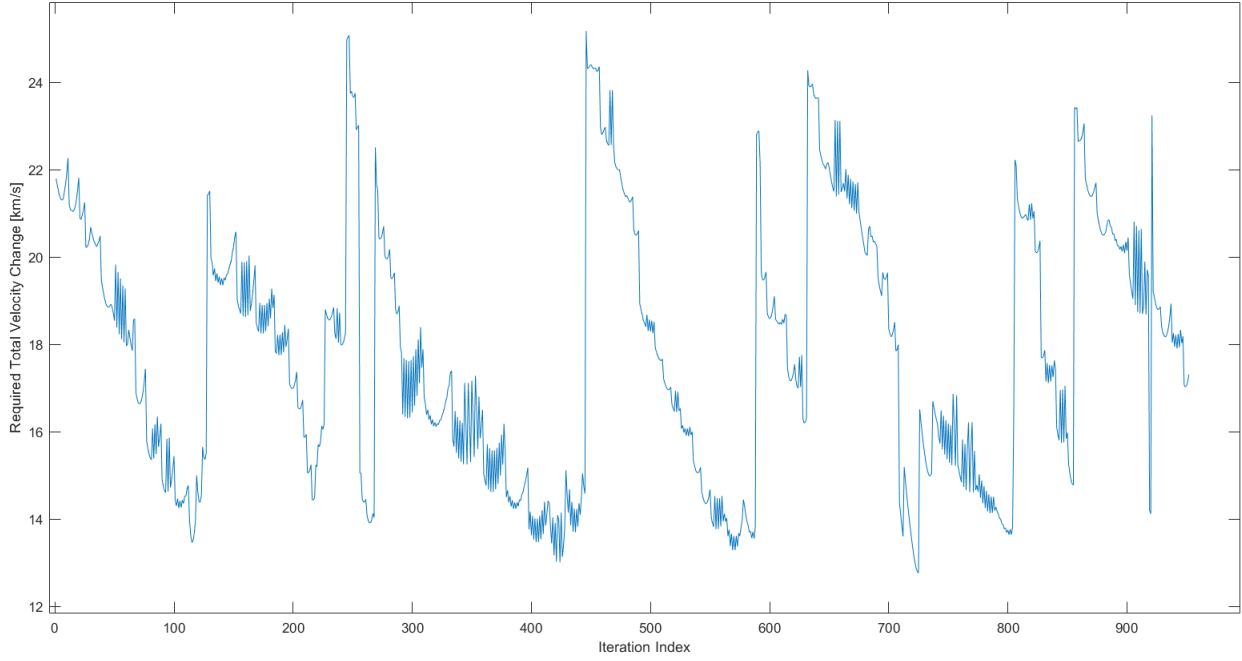


Figure 1.3: The plot of required velocity changes of the trajectory, with respect to the Iteration index.

In the plot of Figure (1.3), many local minima and one absolute minimum are observed. However, because of the 5-day time step and the fact that the two consecutive column indexes do not necessarily correspond to two iterations with only one time-step difference, we cannot conclude that the absolute minimum will be the approximate iteration for the optimum trajectory. Therefore, an optimizer script was developed that with the use of given small time intervals for each one of the departure, flyby, and arrival times, could find the trajectory with the absolute minimum ΔV_{tot} (Fine tuning).

1.4.2 The optimization script

Since the data found from the main script, differ from each other with time steps of five days or more, an optimizer is used to find a more accurate time configuration (consisting of the departure, flyby, and arrival times) around the predefined trajectories. For this matter, two major steps have been taken:

- *Developing a function based off the main script that with the time configuration as its input, will calculate the ΔV_{tot} of the trajectory.*
- *Developing the optimization script to take a time configuration as input and employ the Particle Swarm method that will use the above function with a time interval of 10 days or less around each of the dates of the time configuration. After finding the optimum trajectory through the particle swarm, the script will plot the interplanetary trajectory and the flyby inside the Venus's sphere of influence.*

Several of the local minima, including the absolute minimum, were fed to the optimizer script and between them, the optimum trajectory with minimum ΔV_{tot} was computed. The optimization script ran several

times with smaller and smaller time intervals for each of the dates of the time configuration to provide the trajectory with minimum ΔV_{tot} . A summary of the findings throughout this process is provided in Tables (1.2) and (1.3).

Table 1.2: Summary of the required velocity impulses found during the project.

-	Initial run	2^{nd} run	Final optimization
Minimum ΔV_{tot} [km/s]	14.3	12.9	12.4060

Table 1.3: Details of the optimum trajectory with minimum required velocity change.

-	Earth to Venus	Venus flyby	Venus to Mercury	Total
Time	December 22 nd , 2056	March 27 th , 2057	May 17 th , 2057	<i>ToF = 147 days</i>
Required ΔV [km/s]	$\Delta V_{departure} = 4.2941$	$\Delta V_{flyby} = 0$	$\Delta V_{arrival} = 8.1119$	$\Delta V_{tot} = 12.4060$

1.5 Results analysis

After the optimizations, it is found that the best trajectory with minimum required velocity change for the spacecraft, between the time window of December 1st, 2028 to December 1st, 2068, is when the spacecraft departs from Earth's orbit on December 22nd, 2056, makes a flyby at Venus on March 27th, 2057, and arrives at Mercury on May 17th, 2057.

Having the dates of the optimum trajectory at hand, it is possible to plot the complete trajectory that was designed using the patched conics method and calculate the required velocity change at each step of the way. Since none of the objective planets are in the same orbital plane around the sun, the spacecraft needs to have its first and second heliocentric transfer legs in different planes. The three-dimension view of the optimum trajectory is shown in Figure (1.4). It should be noted that heliocentric inertial frame is used as the main reference frame.

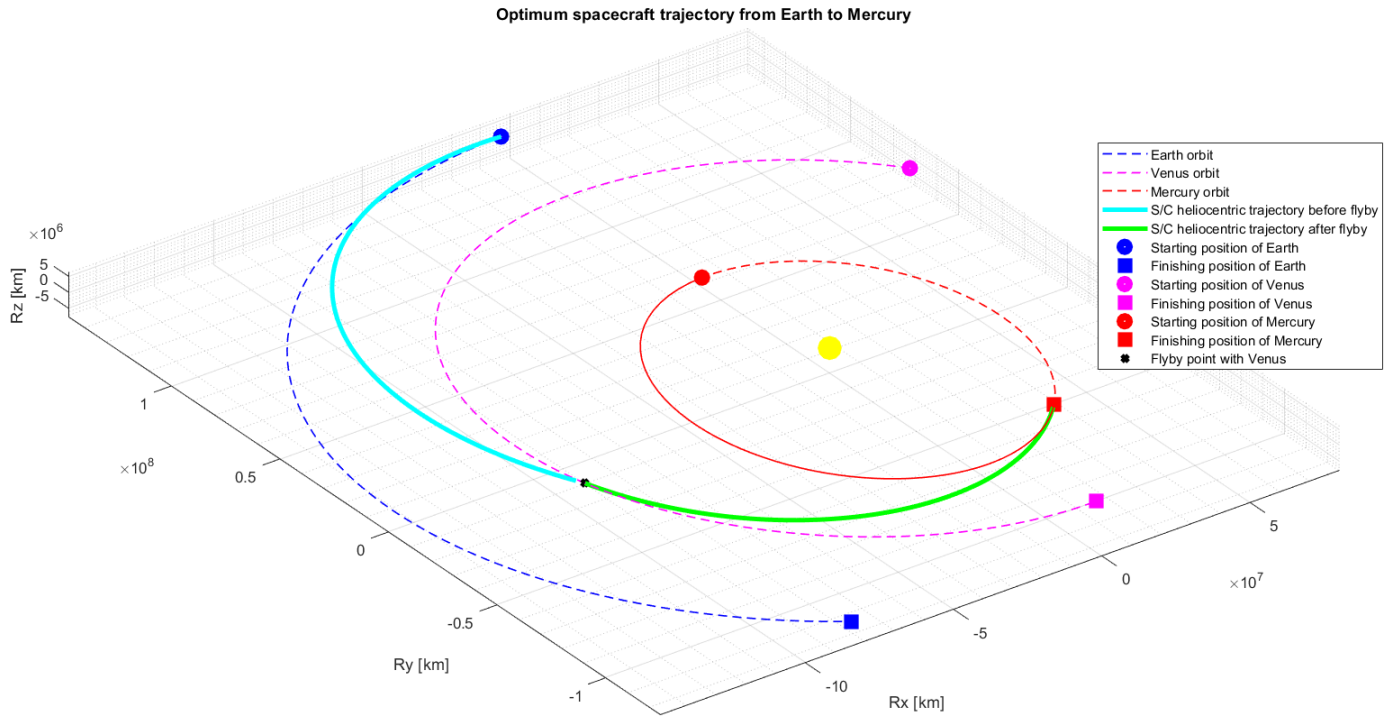


Figure 1.4: The 3D view of the spacecraft's optimum trajectory from Earth to Mercury, with a flyby at Venus.

1.5.1 Departure from planet Earth

On December 22nd, 2056, around 9 AM, the spacecraft is required to decrease its heliocentric velocity to escape from planet Earth's orbit and fly towards Venus. The details of position and velocity of Earth and the spacecraft are as follows:

Table 1.4: Details at the time of departure.

$V_{Earth} = [-30.2644; -0.7589; 0]$ km/s	$r_{Earth-S/C} = [-0.0211; -0.9835; 0]$ AU
$V_{S/C} = [-26.2572; -0.1371; 1.4145]$ km/s	$\Delta V_{First-leg} = [4.0070; 0.6218; 1.4145]$ km/s

1.5.2 Arrival at planet Mercury

On May 17th, 2057, about 3 A.M, the spacecraft arrives at Mercury and will need to decrease its heliocentric velocity to remain on Mercury's orbit. The related details are presented below:

Table 1.5: Details at the time of arrival.

$V_{Mercury} = [27.4958; 33.6258; 0.1598]$ km/s	$r_{Mercury-S/C} = [0.2719; -0.3221; -0.0512]$ AU
$V_{S/C} = [33.7169; 38.7829; 0.8650]$ km/s	$\Delta V_{Second-leg} = [-6.2212; 5.1571; -0.7052]$ km/s

1.5.3 Flyby and Gravity Assist at planet Venus

On March 27th, 2057, about 5 AM, the spacecraft will arrive at Venus with the velocity of $V_{S/C}^-$ and then depart with the velocity of $V_{S/C}^+$. So, the entry and exit velocities of the spacecraft at the edge of the sphere of influence of Venus will be v_∞^- and v_∞^+ respectively. Since the norm of the entry and exit velocities are the same, we understand that this flyby will be a normal gravity assist, without any required velocity change. Therefore, all the characteristics of the hyperbola before and after the close approach, are the same. The radius of the sphere of influence is calculated at the time of flyby. It is observed that the spacecraft makes a very close approach during its flyby and exploits Venus's gravity nearly completely. The periapsis altitude of the flyby hyperbola is calculated to be 162 kilometres, while the maximum atmosphere altitude of Venus was assumed as 100 kilometres. In the real case scenario, there might be some atmospheric drag at this close approach and therefore, a velocity change may be needed. The flyby of the spacecraft at Venus is shown on Figure (1.5) and the summary of the flyby trajectory is provided below:

Table 1.6: Details of the flyby.

$V_{Venus} = [9.1751; -33.8953; -0.9765]$ km/s	$r_{Venus} = [-0.6937; -0.1933; 0.0376]$ AU
$V_{S/C}^- = [17.1697; -32.4457; -0.8873]$ km/s	$V_{S/C}^+ = [13.0431; -27.2229; -3.5337]$ km/s
$v_\infty^- = [7.9946; 1.4496; 0.0891]$ km/s	$v_\infty^+ = [3.8680; 6.6724; -2.5573]$ km/s
$\Delta v_{periapsis} \cong 0$ km/s	$\Delta V_{flyby} = [-4.1266; 5.2228; -2.6464]$ km/s
$\delta = 52.3078^\circ$	$\Delta V_{flyby-norm} = 7.1631$ km/s
$\Delta = 9988$ km	$e_{hyp} = 2.2629$
$a_{hyp} = -4920$ km	$R_{SOI} = 614377$ km
$\theta_{SOI} = 115.2983^\circ$ ($\theta_\infty = 116.2262^\circ$)	$\Delta t_{flyby} = 40.75$ hrs

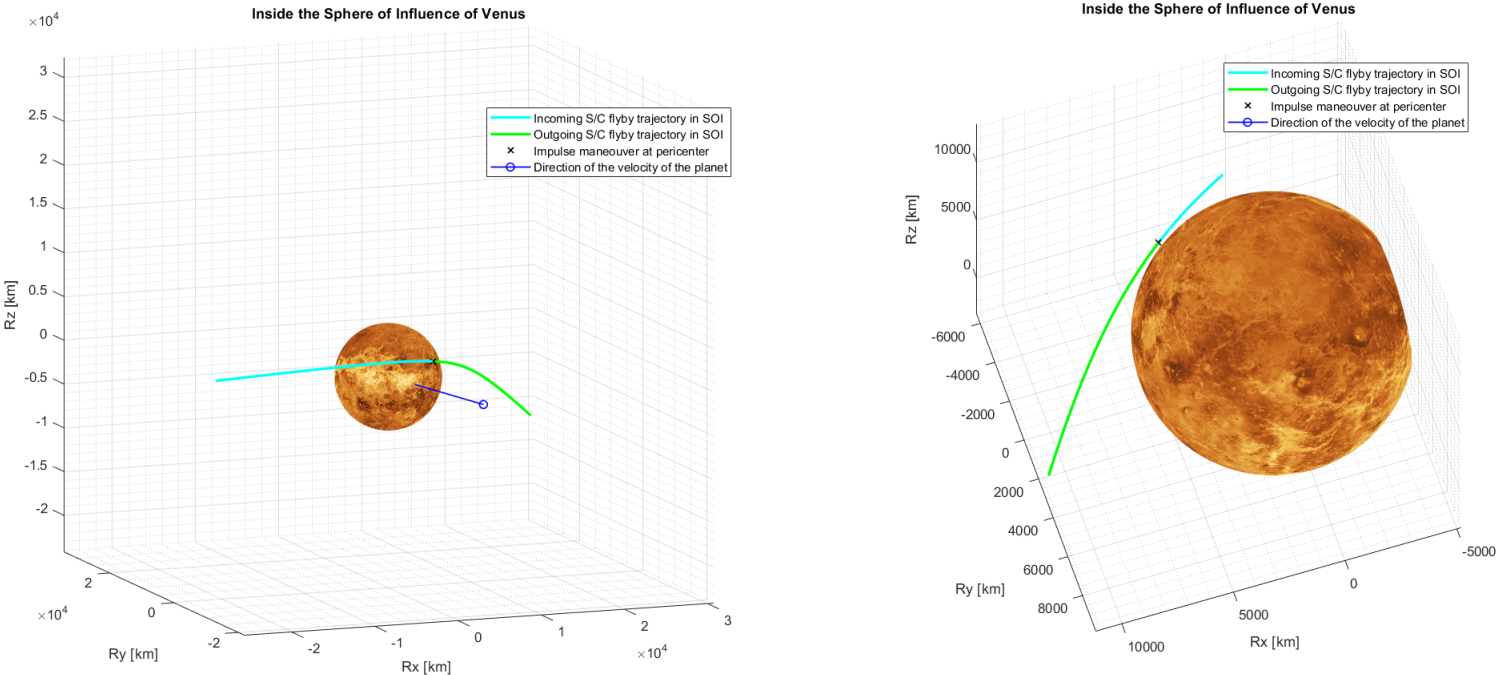


Figure 1.5: The flyby trajectory of the spacecraft at Venus.

2. Planetary Mission Design

The second part of the report focuses on the analysis of orbit grountrack and perturbations. The two problems are going to be discussed separately in the following sections, using as initial conditions the following keplerian parameters:

Table 2.1: Initial keplerian parameters.

	symbol	value	unit measure
Semi-major axis	a	27224	km
Eccentricity	e	0.3161	[−]
Inclination	i	16.2195	deg
RAAN	Ω	8	deg
Argument of perigee	ω	94	deg
True anomaly	θ	0	deg

2.1 Groundtracks analysis

2.1.1 Groundtrack and Earth's oblateness effects

Groundtracks represent the projection of a satellite's orbit on the Earth's surface. The following plot represents the results obtained propagating the initial values (in cartesian coordinates) for one orbital period, without taking into consideration the effects of oblateness (J_2).

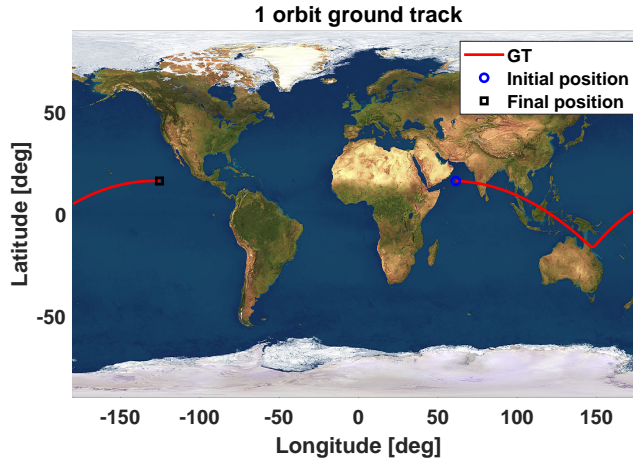


Figure 2.1: 1 T groundtrack with no perturbation.

As it can be observed, the relative trajectory covered by the satellite takes almost two entire orbits to cross again the starting meridian. This depends on the value of the semi-major axis, that fully defines the period of the orbit for the equation $T = 2\pi\sqrt{\frac{a^3}{\mu}}$. The following table reports the orbital period considered and its relation with the sidereal day:

Table 2.2: Periods at comparison.

T_{SAT}	12.9363	hr
T_{Earth}	23.9345	hr
T_{SAT}/T_{Earth}	0.5406	

Let now consider the effects of the J_2 . It introduces a perturbation that over time modifies the orbit and its projection. The more time passes, the more the effect is consistent:

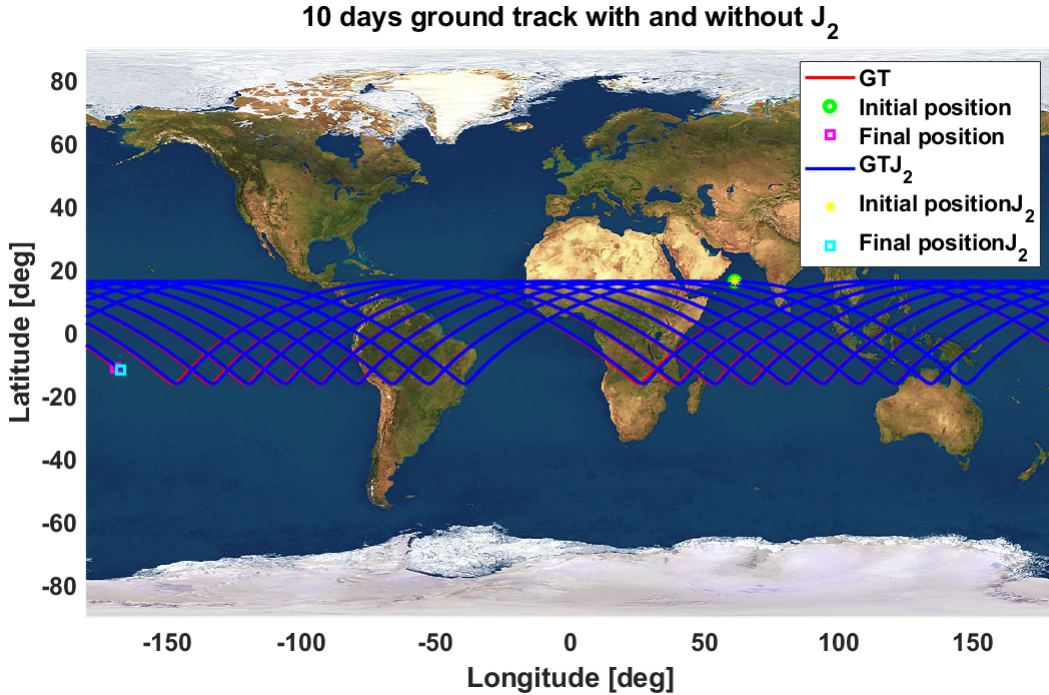


Figure 2.2: 10 days GT, perturbed and unperturbed.

The perturbation effect can be easily seen in the presented plot, particularly in the final position, at the end of the propagation. It can also be noticed that over time the orbit's projection appears translated on the Earth's surface. The reason of this behaviour is that the original periods (Table (2.2)) do not respect the equation [2]:

$$\frac{T_{SAT}}{T_{Earth}} = \frac{m}{k} \quad \text{with} \quad m, k \in N \quad (2.1)$$

Where k is the number of revolutions of the satellite and m is the number of rotations of Earth. Wanting to obtain a repeating groundtrack, it is necessary to modify the value of the semi-major axis of the orbit, so that the ratio is a rational number.

2.1.2 The Repeating Groundtrack

The relation m/k was given as a requirement of the project. The new value of the semi-major axis for the unperturbed case can be found from the required period, while if the oblateness effect is considered the

value of the new a has to be computed numerically with a zero function. The following table reports the values obtained:

Table 2.3: New semi-major axes for RG with $m/k = 0.5$.

Old value	27,224,00 km
RG with no J_2	26,563.02 km
RG with J_2	26,560.98 km

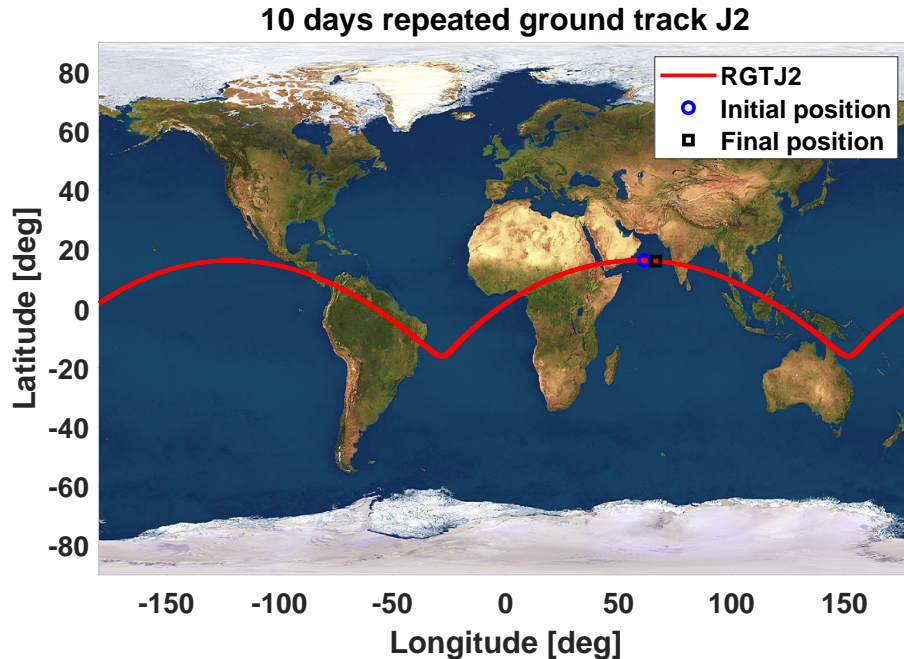


Figure 2.3: 10 days propagation for a Repeated Groundtrack considering oblateness effect.

As it can be seen in the previous figure, obtained using the new semi-major axis, the groundtrack does not present the translation effect. Even considering higher numbers of completed orbital periods, the satellite does not change its projected trajectory pattern.

2.2 Perturbed Orbit Propagation

In this section the effects of Earth's oblateness and solar radiation pressure (SRP) on the spacecraft's orbit keplerian parameters are going to be analysed.

Up until this point, in the previous part of the project, every orbit has been propagated with a cartesian propagation method, based on the position and velocity of the considered bodies in an inertial reference frame (Earth centred or heliocentric). To study the orbit perturbations, also the Gaussian method is going to be used. It allows to directly propagate the keplerian elements, the slight differences between the two methods are going to be presented in the plots.

2.2.1 Perturbed Problem

2.2.1.1 Oblateness Effects

The effects of interest for our analysis due to the oblateness of the Earth are the nodal regression and the perigee precession, that cause the so called "hula-hooping effect". They are function of the inclination, the semi-major axis and eccentricity, that instead are not effected by J_2 [3].

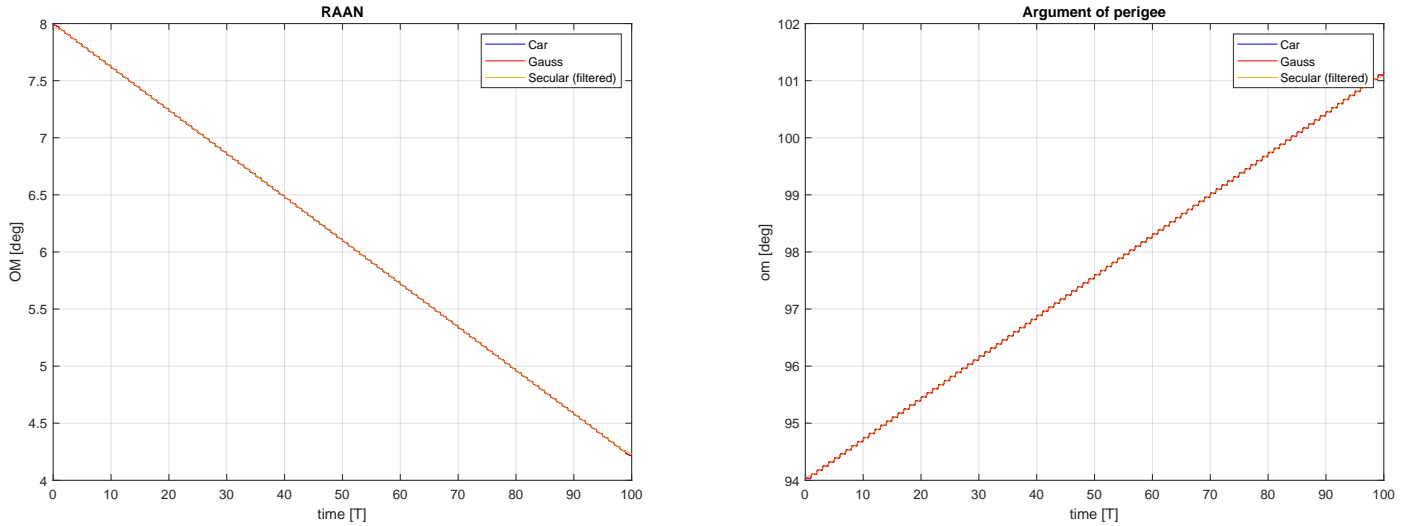


Figure 2.4: Perturbation effects due to Earth's oblateness with propagation for 100 orbits. Cartesian, Gaussian and filtered Gaussian (using movemean filter [4]) are compared. On the left, nodal regression. On the right, perigee precession.

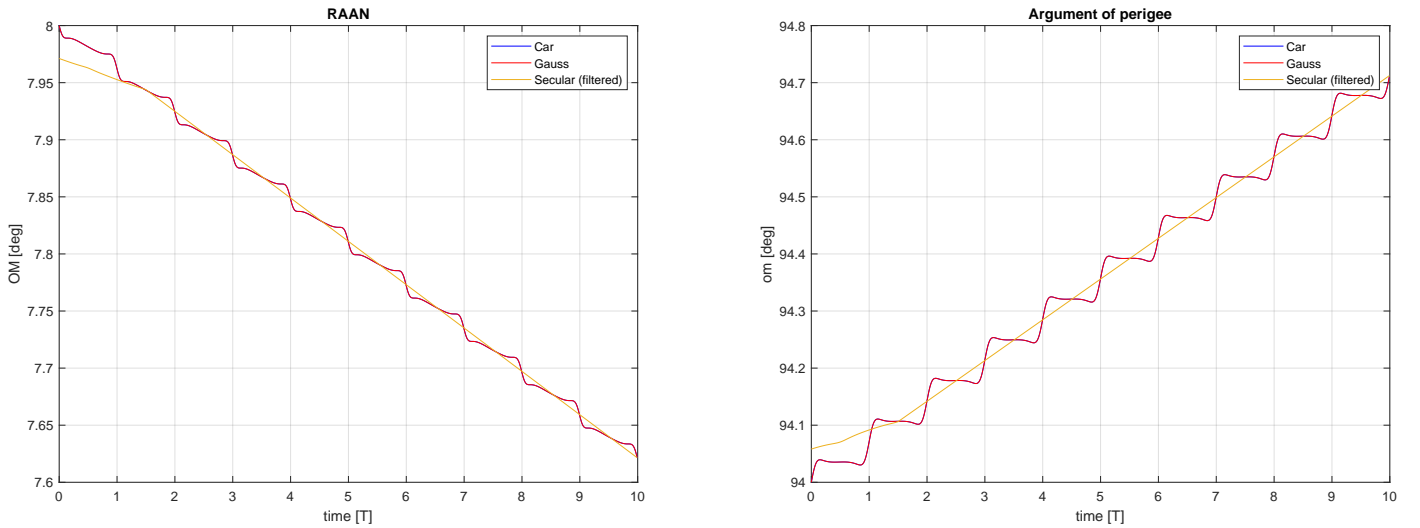


Figure 2.5: Detail of the two previous plots for 10 orbital periods.

2.2.1.2 Solar Radiation Pressure Effects

Differently from Earth's oblateness effect, here considered depending only on J_2 and on the orbital parameters, the SRP perturbation is affected also by some characteristics of the spacecraft and by the relative position between satellite and Sun. In the next table the SRP coefficient and the area to mass ratio considered for the calculations are reported:

Table 2.4: Spacecraft characteristics.

C_R	1
A/m	$1 \text{ m}^2/\text{kg}$

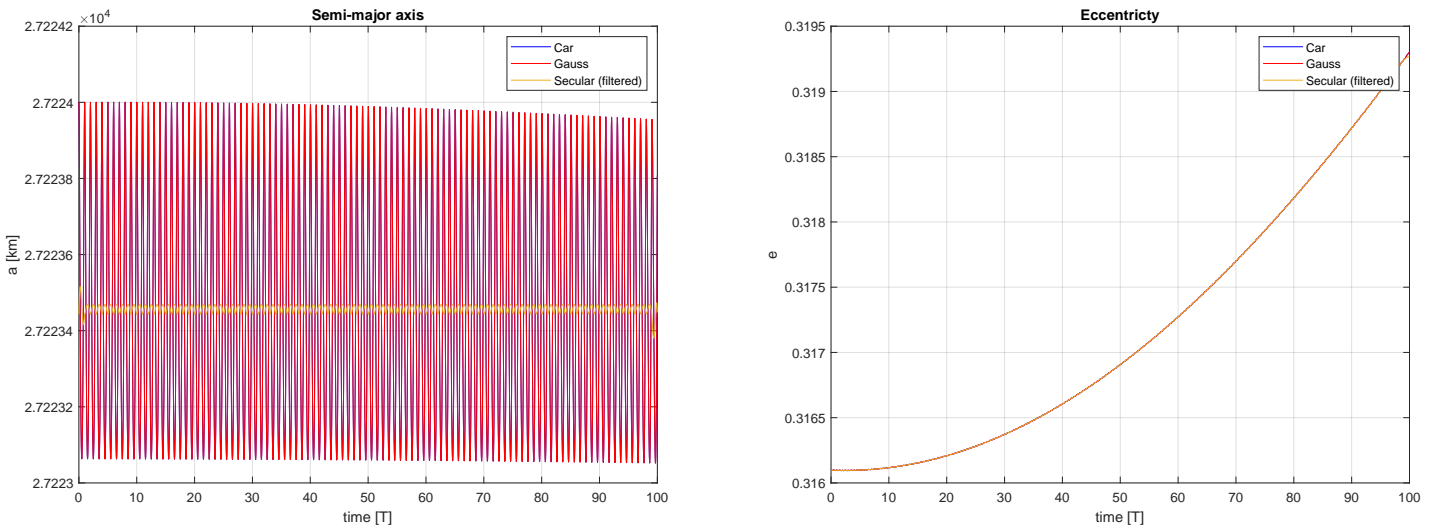


Figure 2.6: Perturbation effect due to solar radiation pressure with propagation for 100 orbits. Cartesian, Gaussian and filtered Gaussian (movemean filter) are compared. On the left, semi-major axis evolution. On the right, eccentricity increasing.

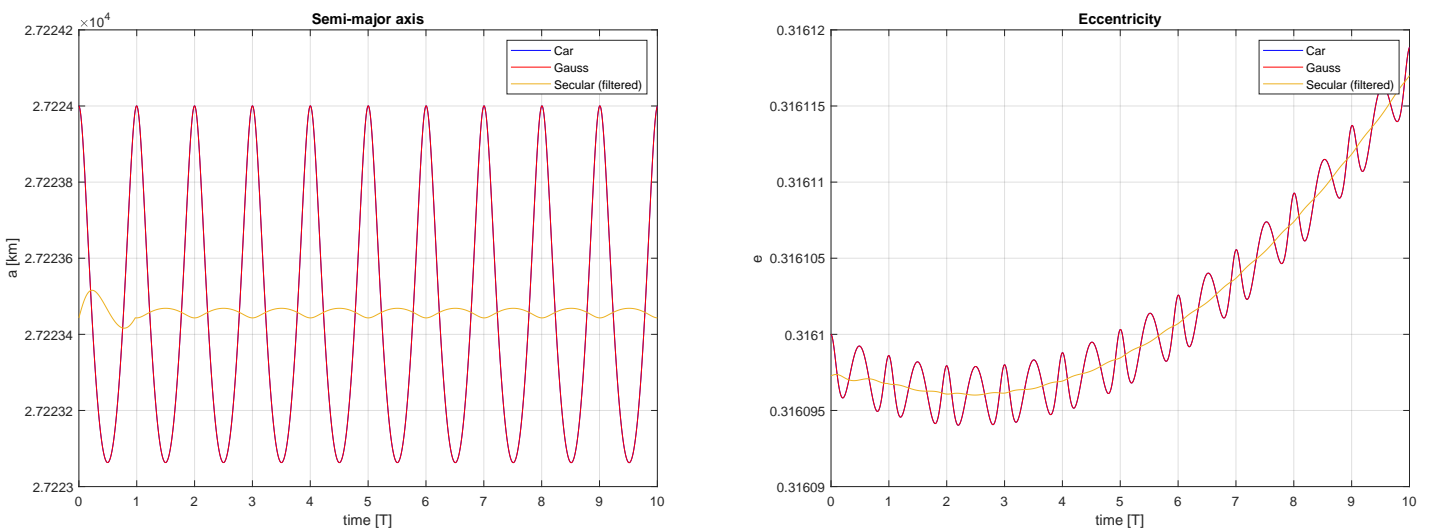


Figure 2.7: Details of the two previous plots for 10 orbit periods.

2.2.2 Combined effects

As it can be reasonably expected, the results obtained considering both perturbations together are just a superposition of the effects.

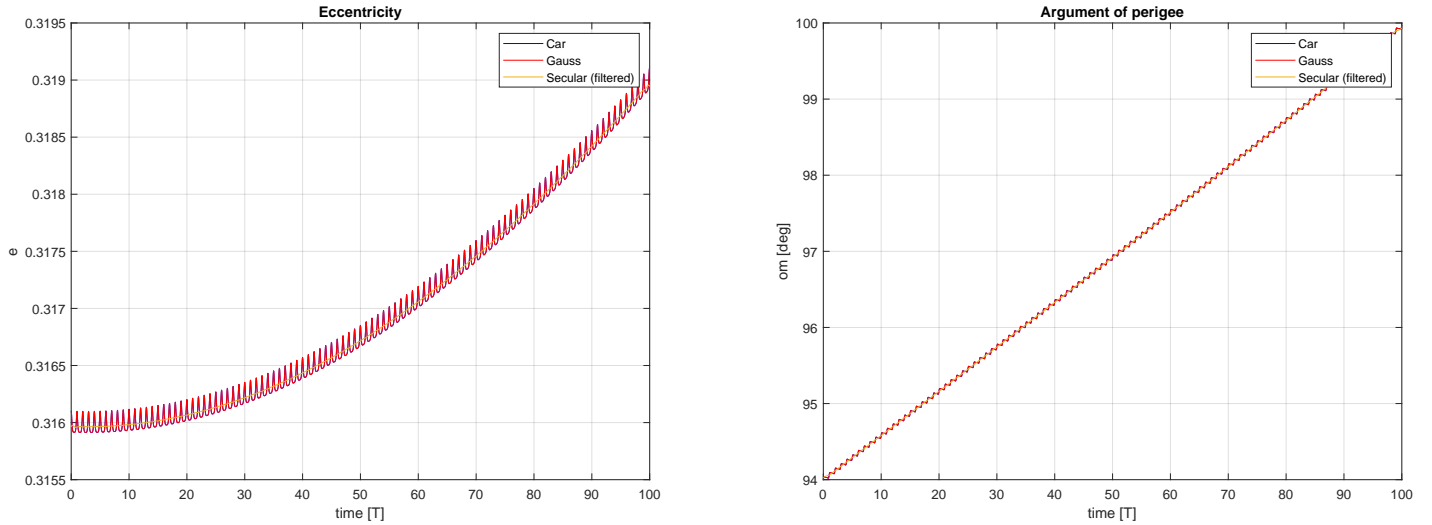


Figure 2.8: Eccentricity (left) and argument of perigee (right) evolution over 100 orbits, accounting for both SRP and J_2 effects. Cartesian, Gaussian and filtered Gaussian (movemeans).

Comparing the two algorithms, the resulting error is of $O(10^{-11})$, so they can be considered accurate in the same way. Moreover, Gaussian propagation is less demanding from the computational point of view.

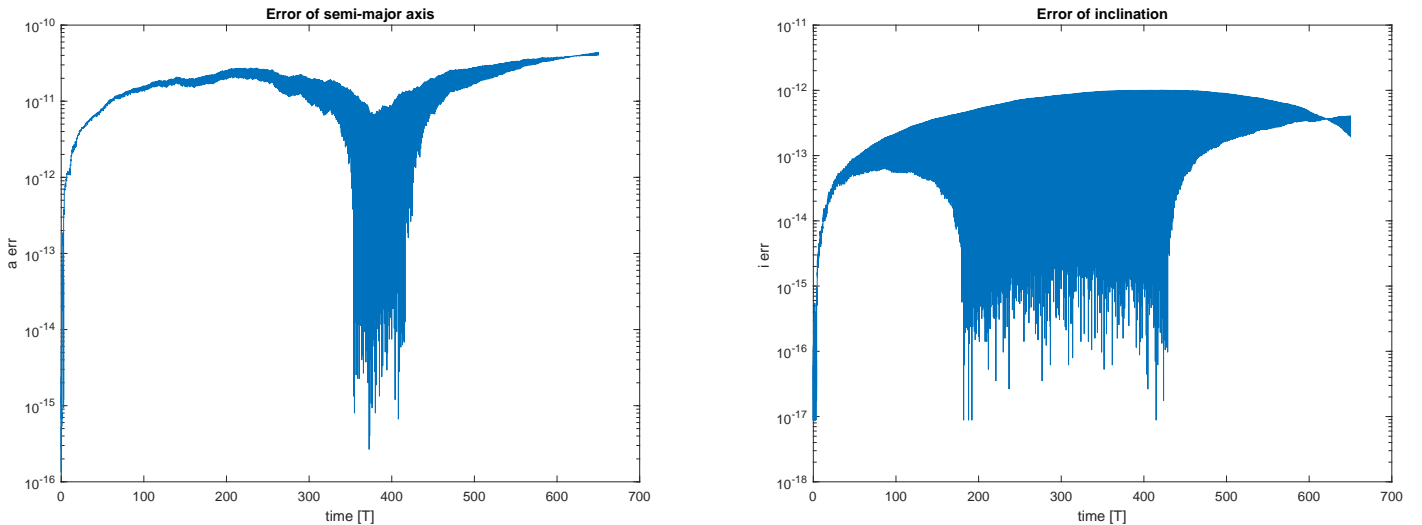


Figure 2.9: Normalized error for semi-major axis, on the left, and inclination, on the right, between Gaussian and cartesian propagation methods.

2.3 Comparison with Real Data

To assess the reliability of the adopted models they can be used to obtain the evolution of the orbit of a real satellite, of which the ephemerides are known from the TLE available online [5] and then compare the results. The chosen spacecraft for the procedure is Galileo 5 (NORAD CAT ID=40128) since it is in a relatively similar orbit. The presented comparisons are going to use alternatively Gauss' or cartesian propagation, since the results are almost identical.

Table 2.5: Initial orbit elements.

	symbol	value	unit measure
semi-major axis	a	27977	km
eccentricity	e	0.1662	[−]
inclination	i	50.5813	deg
RAAN	Ω	8.0834	deg
argument of perigee	ω	93.9227	deg
true anomaly	θ	143.1312	deg

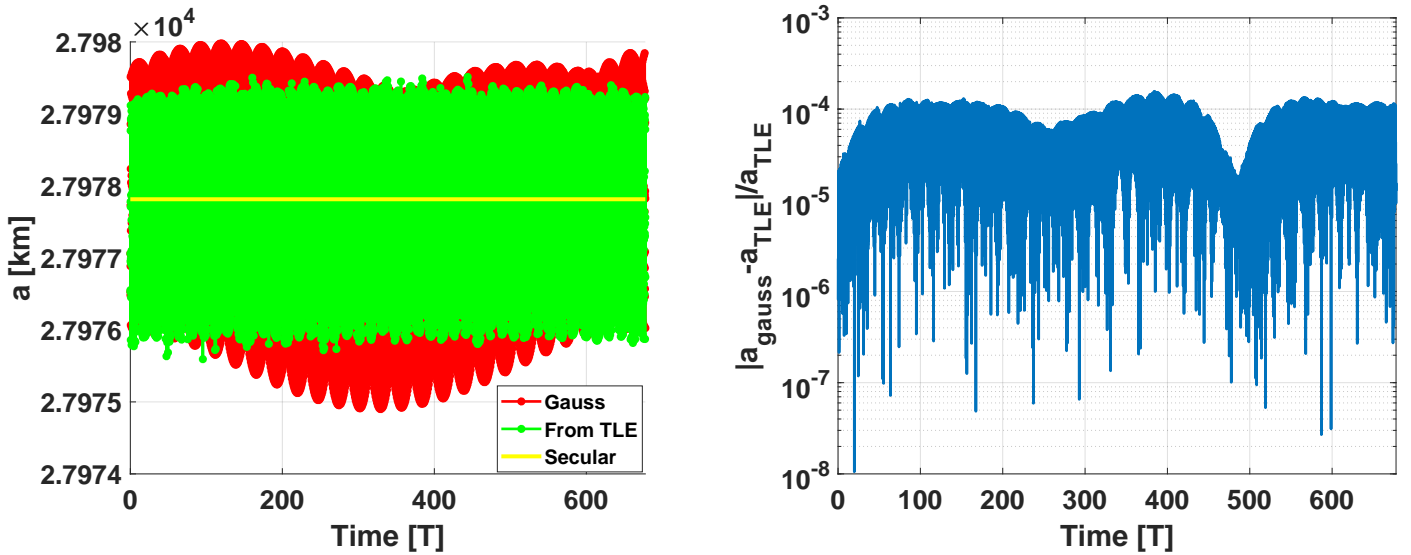


Figure 2.10: Evolution of semi-major axis, real and Gauss (left) and normalised error between the two (right).

The period considered for the analysis is one entire year, this is because the effects of SRP vary over this period. During this time the satellite completes more than 600 orbits around the Earth and, as one can see in the reported graphs, the value of the semi-major axis is practically constant, changing of a few kilometres at maximum. The error between the real data and the propagated values is satisfying and in the order of $O(10^{-4})$ or lower.

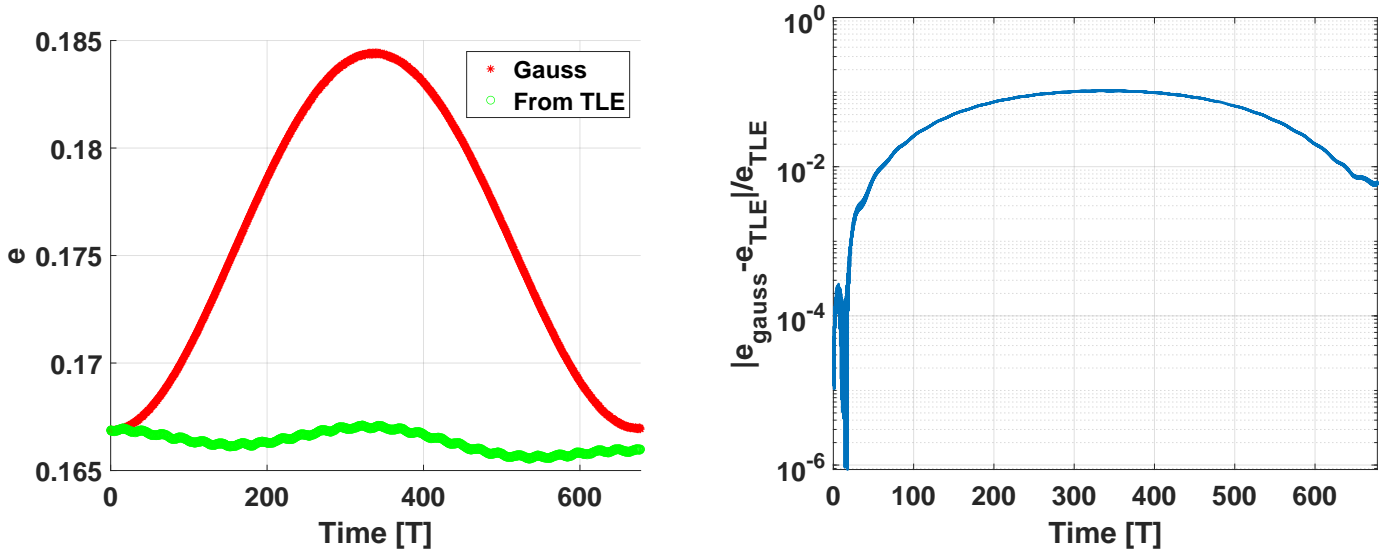


Figure 2.11: Evolution of eccentricity, real and Gauss (left) and normalised error between the two (right).

The plot of the eccentricity presents a significant difference between the propagated and the real data. The value obtained from the propagated values follows the expected pattern due to the effects of SRP during a year, instead the eccentricity of the real satellite has very low excursion. It's legitimate to assume that the error is due to the different spacecraft characteristics, the perturbations not considered by the model and, mostly, the active orbit control performed by the real satellite to remain on the objective orbit.

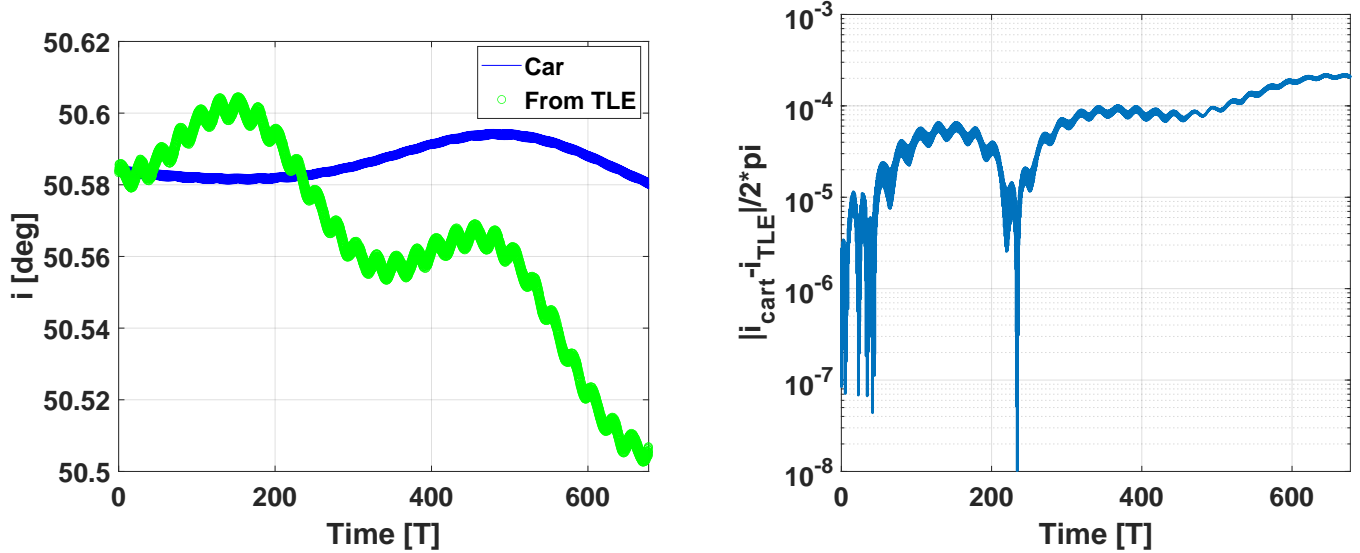


Figure 2.12: Evolution of inclination, real and cartesian, on the left, and normalised error between the two, on the right.

As the graphs depict, the inclination of the real spacecraft changes slightly more than the value obtained with the propagation, but still the error is acceptable, and likely caused by the considerations presented above.

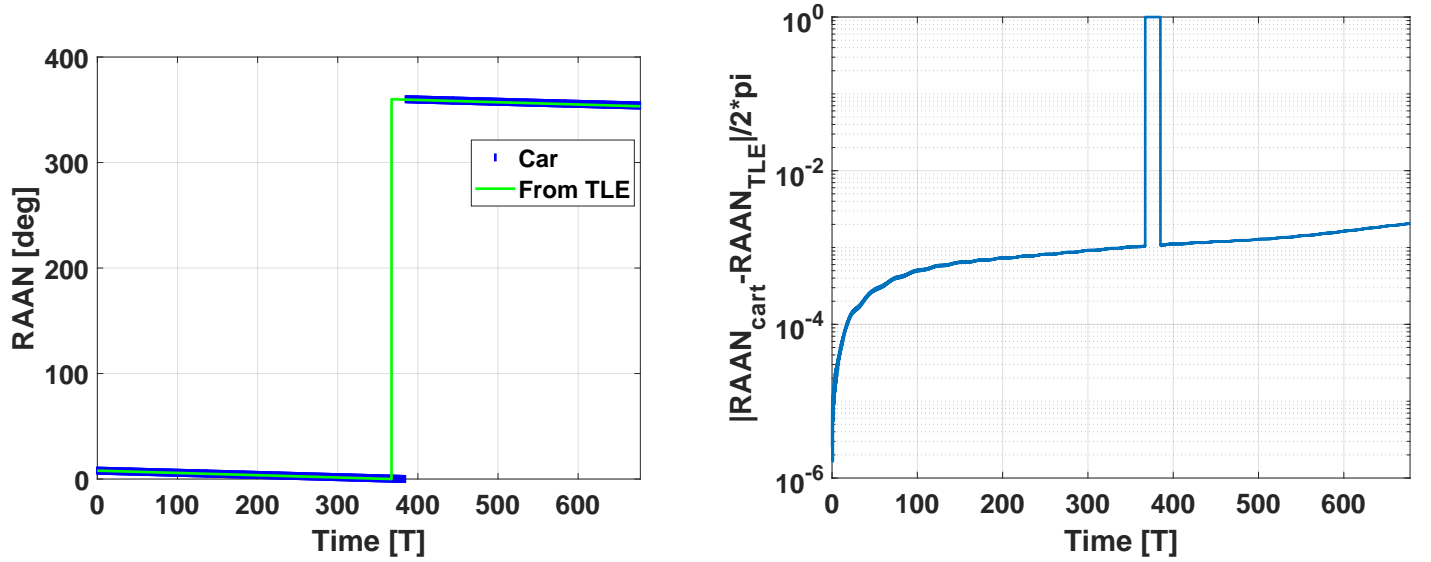


Figure 2.13: Evolution of RAAN, real and cartesian (left) and normalised error between the two (right).

The RAAN evolution is of particular interest because of the change of sign of the real data after 367 orbits. The delay in the change of sign in the propagation is what causes the spike in the error's plot, that soon after the change returns to an acceptable value in the order of $O(10^{-2})$.

3. Conclusions

The procedure reported in the first chapter of the report found a suitable trajectory to perform the required mission minimizing the ΔV and also obtaining a low value of ToF. It is needless to say that many other possible solutions exist, that could involve more than one revolution around the Sun (increasing inevitably the ToF) and different choices for the gravity assists, that could be multiple and also around Earth and Mercury. A comparison can be made with ESA's BepiColombo mission to Mercury, its flight profile involves 8 different gravity assists, 17 orbits around the Sun and almost 7 years to reach the planet and thus, required less velocity change but without complying to the requirements of one Venus's fly-by [6]. It should also be noted that the amount of time spent in the sphere of influence of Venus is high with respect to the total time of flight of the trajectory. Therefore, the method of patched conics may not be a very good assumption and more accurate methods should be used for a better preliminary design.

The scripts and functions developed in the second chapter for the various propagations of groundtracks and orbital perturbations give extremely good results with low error, in line with those expected from the knowledge of theory. Obviously the differences between the real space environment, celestial bodies and spacecraft have to be kept in mind. In order to obtain better results, a finer model would be needed and it would have to take into account other aspects such as:

- the other perturbations and their real (not modeled) values;
- the spacecraft's orbit control system;
- the real conformation of the satellite considered.

4. References

- [1] *Planetary fact sheet*
(<https://nssdc.gsfc.nasa.gov/planetary/factsheet>)
- [2] *Module 2 - Orbit representation, Juan Luis Gonzalo Gomez, Giacomo Borelli, Camilla Colombo, A.Y.2020/21*
- [3] *OrbMech-05-OrbitPerturbations, Dr Camilla Colombo, Orbital Mechanics course, A.Y.2020/21*
- [4] *Module 5 - Orbit perturbations, Juan Luis Gonzalo Gomez, Giacomo Borelli, Camilla Colombo, A.Y.2020/21*
- [5] *NASA Horizons for real ephemerides*
(<https://ssd.jpl.nasa.gov/horizons.cgi#top>)
- [6] *The BepiColombo Spacecraft and its mission to Mercury*
(<https://www.hou.usra.edu/meetings/lpsc2015/eposter/1058.pdf>)